2005 American Control Conference
June 8-10, 2005. Portland, OR, USA

Generation of a Vibration Suppression Control Profile from Optimal Energy Concentration Functions

Li Zhou and Eduardo A. Misawa

Abstract— **A reference trajectory is generated which suppresses all the high frequency resonant dynamics in a flexible dynamic system. This reference trajectory is based on the shifted prolate spheroidal wave function that optimally achieves the energy concentration property. The reference trajectory is optimized by considering the first resonance frequency through the filter theory. The simulation results of hard disk drive actuator position control illustrate the effectiveness of the proposed method.**

I. Introduction

Control of flexible structures has been extensively studied in recent years. Flexible structures such as high-speed disk drive actuators require extremely precise positioning under very tight time constraints. Whenever a fast motion is commanded, residual vibration in the flexible structure is induced, which increases the settling time. One solution is to design a closed-loop controller to damp out vibrations caused by the command inputs and disturbances to the plant. However, the resulting closed-loop response may still be too slow to provide an acceptable settling time, and the closed-loop control is not able to compensate for high frequency residual vibration which occurs beyond the closed-loop bandwidth. An alternative approach is to develop an appropriate reference trajectory that is able to minimize the excitation energy imparted to the system at its natural frequencies.

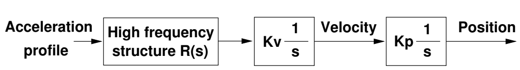

Fig. 1. A typical mechanical flexible system.

Fig. 1 shows a typical mechanical flexible system, where $\frac{1}{s}$ is an integrator, K_v is a velocity constant gain, and K_p is a position constant gain. The high frequency modes can be described as a transfer function $R(s) = \lim_{n\to\infty} \frac{b_n s^n + b_{n-1}s^{n-1}+\cdots+b_1 s+1}{a_n s^n + a_{n-1}s^{n-1}+\cdots+a_1 s+1}$ in which an infinite number of lightly damped resonant structures is possible. The goal of vibration suppression trajectory generation is to find a fast input trajectory, under some physical constraint, with minimum possible residual vibration.

This work was supported by the National Science Foundation, grant number 9978748, and Seagate Technology LLC of Oklahoma City, Oklahoma.

L. Zhou is with the School of Mechanical and Aerospace Engineering, Oklahoma State University, Stillwater, OK 74078-5016, USA zhoul@acl.okstate.edu

E. A. Misawa is with Faculty of School of Mechanical and Aerospace Engineering, Oklahoma State University, Stillwater, OK 74078-5016, USA misawa@ceat.okstate.edu

To suppress all the high frequency resonant dynamics in a flexible system, Zhou and Misawa [1] have proposed robust vibration suppression reference trajectory generation based on time-frequency uncertainty. An optimal shifted time-limited discrete-time Gaussian function is derived to maximize the proportion of its energy before the first resonance frequency. Suppose a continuous-time filter $f(t)$ is to have a finite support impulse response defined only on $0 \le t \le T$. Also, as much of the impulse response energy as possible is contained in $|\omega| \le \Omega$, i.e.,

$$\max_{f(t)} \frac{\int_{-\Omega}^{\Omega} |F(\omega)|^2 d\omega}{\int_{-\infty}^{\infty} |F(\omega)|^2 d\omega}, \tag{1}$$

where $F(\omega) = \int_0^T f(t)e^{-i\omega t}dt$ is the Fourier transform of $f(t)$. Here, the detail on the function $f(t)$ is not known and it can be an arbitrary energy bounded signal. Slepian and his colleagues at Bell Labs in 1961 found that the shifted prolate spheroidal wave functions are the solutions for the problem [2], [3], [4], [5]. In this paper, vibration suppression profile generation using prolate spheroidal wave functions will be examined.

Instead of using concentration in the sense of Heisenberg uncertainty, Slepian et al. introduced a more meaningful measure of a signal for the communication engineer

$$\alpha^2(T) := \frac{\int_{-T/2}^{T/2} |f(t)|^2 dt}{\int_{-\infty}^{\infty} |f(t)|^2 dt}, \tag{2}$$

i.e., the fraction of the signal's energy that lies in the time interval $[-T/2, T/2]$. Similarly,

$$\beta^2(\Omega) := \frac{\int_{-\Omega}^{\Omega} |F(\omega)|^2 d\omega}{\int_{-\infty}^{\infty} |F(\omega)|^2 d\omega} \tag{3}$$

is a measure of energy concentration of the amplitude spectrum of $f(t)$. Here ":=" denotes "equal to by definition."

Slepian's original question was to determine how large $\alpha^2(T)$ can be for $f(t)$ in the space of band-limited signals. The group found the prolate spheroidal wave functions were exactly the solutions to the original problem. In short, given any $T > 0$ and any $\Omega > 0$, the original problem has a countably infinite set of functions $\psi_0(t), \psi_1(t), \psi_2(t), \ldots$ and a set of corresponding $\lambda_i = \alpha^2(T), i = 0, 1, 2, \ldots$, such that $\lambda_0 > \lambda_1 > \lambda_2 > \ldots$. The best choice of $f(t)$ satisfying (1) is the zeroth order shifted prolate spheroidal wave function $f(t) = \psi_0(t + T/2, c)$, where $c = \Omega T/2$.

The waveform ψ_0 can be used to generate a reference velocity candidate to suppress all the high frequency vibrations with the energy concentration objective (1). Since the waveform of the reference velocity is known, the acceleration, jerk, position and other profiles can be derived to synthesize the control input signals to suppress the residual vibration in a flexible system.

II. Energy Concentration Problem in Discrete-Time Case

In this section, the energy concentration problem in the discrete-time case is studied. The results for this case were originally derived by Slepian [6]. Let $\{h[k]\} = \ldots, h[-1], h[0], h[1], \ldots$ be a real or complex valued sequence with finite energy. The discrete-time Fourier transform of $h[k]$ is $H(f) = \sum_{k=-\infty}^{\infty} h[k]e^{-j2\pi fk}$, $H(f)$ is a periodic function in f with period 1. The discrete-time sequence $\{h[k]\}$ has the following representation: $h[k] = \int_{-1/2}^{1/2} H(f)e^{j2\pi fk}df$. The energy of the sequence $\{h[k]\}$ in the index interval $[n_1, n_2]$ is denoted as $E(n_1, n_2) := \sum_{k=n_1}^{n_2} |h[k]|^2$, and the total energy is denoted as $E := E(-\infty, \infty) = \sum_{k=-\infty}^{\infty} |h[k]|^2$.

It is natural to ask how large the fraction of the energy in the index range from 0 to $N-1$ can be for a band-limited sequence, i.e., to determine the maximum value of

$$\alpha^2(N) := \frac{E(0, N-1)}{E(-\infty, \infty)} = \frac{\sum_{k=0}^{N-1} |h[k]|^2}{\sum_{k=-\infty}^{\infty} |h[k]|^2} \quad (4)$$

for all band-limited sequences with bandwidth $W < 1/2$.

Similarly, an optimal sequence is to be determined to maximize the fraction of the energy in the frequency range $|f| \leq W < 1/2$, i.e., to determine the maximum value of

$$\beta^2(W) := \frac{\int_{-W}^{W} |H(f)|^2 df}{\int_{-1/2}^{1/2} |H(f)|^2 df} \quad (5)$$

for all sequence $\{h[k]\}$ index-limited to $[0, N-1]$. A sequence is index-limited to the interval $[n_1, n_2]$ if $h[k] = 0$ for $k < n_1$ and $k > n_2$.

For the problem of (4), the concentration measure $\alpha^2(N)$ can be written as

$$\begin{aligned}\alpha^2(N) &= \frac{\sum_{k=0}^{N-1} h[k]\overline{h[k]}}{\sum_{k=-\infty}^{\infty} |h[k]|^2}, \\ &= \frac{\sum_{k=0}^{N-1} \int_{-W}^{W} H(f)e^{j2\pi fk}df \int_{-W}^{W} \overline{H(f')}e^{-j2\pi f'k}df'}{\int_{-W}^{W} |H(f)|^2 df}, \\ &= \frac{\int_{-W}^{W} H(f)df \int_{-W}^{W} \overline{H(f')}df' \sum_{k=0}^{N-1} e^{j2\pi(f-f')k}}{\int_{-W}^{W} |H(f)|^2 df}.\end{aligned}$$

By defining $H(f) := G(f)e^{-j\pi f(N-1)}$,

$$\alpha^2(N) = \Big\{ \int_{-W}^{W} G(f)df \int_{-W}^{W} \overline{G(f')}df' e^{-j\pi(f-f')(N-1)} \sum_{k=0}^{N-1} e^{j2\pi(f-f')k} \Big\} \Big/ \int_{-W}^{W} |G(f)|^2 df.$$

Since $e^{-j\pi(f-f')(N-1)} \sum_{k=0}^{N-1} e^{j2\pi(f-f')k} = e^{-j\pi(f-f')(N-1)} \frac{1-e^{j2\pi(f-f')N}}{1-e^{j2\pi(f-f')}} = \frac{e^{-j\pi(f-f')N}}{e^{-j\pi(f-f')}} \frac{1-e^{i2\pi(f-f')N}}{1-e^{i2\pi(f-f')}} = \frac{e^{-j\pi(f-f')N} - e^{j\pi(f-f')N}}{e^{-j\pi(f-f')} - e^{j\pi(f-f')}} = \frac{\sin(\pi N(f-f'))}{\sin(\pi(f-f'))}$, $\alpha^2(N)$ is reduced to the following form

$$\alpha^2(N) = \frac{\int_{-W}^{W} \int_{-W}^{W} \frac{\sin(\pi N(f-f'))}{\sin(\pi(f-f'))} G(f)\overline{G(f')}df df'}{\int_{-W}^{W} |G(f)|^2 df}. \quad (6)$$

Here, $G(f)$ is an arbitrary energy bounded function in $(-W, W)$, and all functions $G(f)$ that maximizes $\alpha^2(N)$ must satisfy the following integral equation [7]

$$\int_{-W}^{W} \frac{\sin(\pi N(f-f'))}{\sin(\pi(f-f'))} \psi(f')df' = \lambda\psi(f), \ |f| \leq W. \quad (7)$$

Since the kernel in the above homogeneous Fredholm equation of the second kind [7] is degenerate. It has only N non-zero distinct, real and positive eigenvalues and they can be ordered such that $1 > \lambda_0(N, W) > \lambda_1(N, W) > \ldots > \lambda_{N-1}(N, W) > 0$.

There are N linearly independent real eigenfunctions of (7) corresponding to these eigenvalues and they are denoted as $U_0(N, W; f)$, $U_1(N, W; f)$, …, $U_{N-1}(N, W; f)$. Here, eigenfunctions that differ only by an arbitrary non-zero multiplicative constant is considered as one eigenfunction. They are called the discrete prolate spheroidal wave functions (DPSWF's). $U_k(N, W; f)$ can be extended to $[-1/2, 1/2]$ from (7), so the DPSWF's $U_k(N, W; f)$ and their corresponding eigenvalues $\lambda_k(N, W)$ are defined by

$$\begin{aligned}&\int_{-W}^{W} \frac{\sin(\pi N(f-f'))}{\sin(\pi(f-f'))} U_k(N, W; f')df' \\ &= \lambda_k(N, W)U_k(N, W; f), \quad k = 0, 1, \cdots, N-1. \quad (8)\end{aligned}$$

The DPSWF $U_k(N, W; f)$ has exactly k zeros in $[-W, W]$ and $N-1$ zeros in $[-1/2, 1/2]$. It is even function if k is even and odd function if k is odd. The band-limited sequence that maximizes $\alpha^2(N)$ in (4) is $h[k] = \int_{-W}^{W} U_0(N, W; f)e^{j2\pi fk}e^{j\pi f(N-1)}df, k = \cdots, -1, 0, 1, \cdots$. With a normalization factor $1/\lambda_0(N, W)$, the following discrete sequence is generated

$$v_0[k](N, W) = \frac{1}{\lambda_0(N, W)} \int_{-W}^{W} U_0(N, W; f) e^{j2\pi fk}e^{j\pi f(N-1)}df, \ k = \cdots, -1, 0, 1, \cdots.$$

The normalization factor $\frac{1}{\lambda_0(N,W)}$ follows Slepian's notation [6] and can be replaced by an arbitrary constant. $v_0[k]$ is called zeroth order discrete prolate spheroidal sequence (DPSS). The n^{th} order DPSS following Slepian's notation [6] can be generated by

$$v_n[k](N, W) = \frac{1}{\epsilon_n\lambda_n(N, W)} \int_{-W}^{W} U_n(N, W; f) e^{j2\pi fk}e^{j\pi f(N-1)}df, \ n = 0, 1, \cdots, N-1,$$

where $\epsilon_n = 1$, if n is even and $\epsilon_n = \sqrt{-1}$, if n is odd.

Slepian [6] notes that the DPSS's also satisfy the following system of equations

$$\sum_{k'=0}^{N-1} \frac{\sin(2\pi W(k-k'))}{\pi(k-k')} v_n[k'](N,W)$$
$$= \lambda_n(N,W)v_n[k](N,W),\ n,k = 0,1,\cdots,N-1. \quad (9)$$

This is to say that $\lambda_n(N,W)$, $n = 0,1,\ldots,N-1$ are the eigenvalues of the $N \times N$ matrix A, where the $(k,k')^{th}$ element of A matrix is given by

$$A_{k,k'} := \frac{\sin(2\pi W(k-k'))}{\pi(k-k')},\ k,k' = 0,1,\cdots,N-1. \quad (10)$$

The eigenvector of matrix A corresponding to the n^{th} eigenvalue $\lambda_n(N,W)$ is exactly the DPSS $v_n[k](N,W)$ with indices from $k=0$ to $k=N-1$, namely $v_n[0](N,W)$, $v_n[1](N,W)$, …, $v_n[N-1](N,W)$.

Now with the results of the first concentration problem in (4) available, the concentration problem (5) for index-limited sequences is studied. If a sequence $h[k]$ is index-limited to the interval $[0,N-1]$, the discrete-time Fourier transform of the index-limited sequence is $H(f) = \sum_{k=0}^{N-1} h[k]e^{-j2\pi fk}$.

The concentration measure in (5) can be computed as

$$\begin{aligned}\beta^2(W) &= \frac{\int_{-W}^{W} H(f)\overline{H(f)}df}{\sum_{k=0}^{N-1}|h[k]|^2},\\ &= \frac{\int_{-W}^{W}\sum_{k=0}^{N-1}h[k]e^{-j2\pi fk}\sum_{k'=0}^{N-1}\overline{h[k']}e^{j2\pi fk'}df}{\sum_{k=0}^{N-1}|h[k]|^2},\\ &= \frac{\sum_{k=0}^{N-1}\sum_{k'=0}^{N-1}h[k]\overline{h[k']}\int_{-W}^{W}e^{j2\pi f(k'-k)}df}{\sum_{k=0}^{N-1}|h[k]|^2},\\ &= \frac{\sum_{k=0}^{N-1}\sum_{k'=0}^{N-1}h[k]\frac{\sin(2\pi W(k-k'))}{\pi(k-k')}\overline{h[k']}}{\sum_{k=0}^{N-1}|h[k]|^2}.\end{aligned}$$

For a real valued sequence $h[k]$, $\beta^2(W)$ can be written as (Percival [8], page 122) $\beta^2(W) = \frac{\mathbf{h}^TA\mathbf{h}}{\mathbf{h}^T\mathbf{h}}$, or $\mathbf{h}^TA\mathbf{h} = \beta^2(W)\mathbf{h}^T\mathbf{h}$, where $\mathbf{h}^T := \begin{bmatrix} h[0] & h[1] & \ldots & h[N-1]\end{bmatrix}$ and A is a $N \times N$ matrix defined in (10). Differentiate both sides of $\mathbf{h}^TA\mathbf{h} = \beta^2(W)\mathbf{h}^T\mathbf{h}$, and the sequence $h[k], k = 0,1,\ldots,N-1$, that maximizes $\beta^2(W)$ must satisfy $A\mathbf{h} = \lambda(N,W)\mathbf{h}$ or $\sum_{k'=0}^{N-1}\frac{\sin(2\pi W(k-k'))}{\pi(k-k')}h[k'] = \lambda(N,W)h[k]$. This equation is exactly equivalent to (9) that describes the zeroth order to $(N-1)^{th}$ order DPSS with indices from 0 to $N-1$. The index-limited sequence that maximizes $\beta^2(W)$ is exactly the zeroth order DPSS, $v_0[k]$, $k = 0,1,\ldots,N-1$.

It is already known that DPSS and its concentration measure can be computed from the eigenvectors and eigenvalues of a $N \times N$ symmetric matrix whose element is described in (10). Percival and Walden [8] compared other computation methods of DPSS's when studying multi-taper spectra analysis. They proposed ([8], page 390, Exercise [8.1]) an efficient way in (11) to compute the eigenvalue $\lambda_n(N,W)$ in (9) given the n^{th} order DPSS $v_n[k]$, $k = 0,1,\ldots,N-1$, is given.

$$\lambda_n(N,W) = 2\left(W\cdot q_0 + 2\sum_{\tau=1}^{N-1}\frac{\sin(2\pi W\tau)}{\pi\tau}q_\tau\right), \quad (11)$$

where $q_\tau := \sum_{k=0}^{N-\tau-1} v_n[k](N,W)v_n[k+\tau](N,W)$. The derivation of (11) can be found in Zhou [9].

In the Matlab Signal Processing Toolbox [10], there is a routine *dpss(n, n * W)* to generate the DPSS's of length n, where W is the normalized half-bandwidth and $0 \le W < 1/2$. It can be directly used here to generate a robust vibration suppression profile based on the idea described in this paper.

III. Robust Vibration Suppression Control Profile Design

In this section, robust vibration suppression control profile generation based on discrete prolate spheroidal sequences are studied. Assume that the frequency bandwidth to be $\Omega_0 = 9.68\times10^3$ rad/sec (the first resonance frequency of a disk drive model in Section IV), the move time (the time duration of the feed forward control input, such as acceleration) of the DPSS is chosen to be 1.5×10^{-3} sec, and the sampling period of the discrete sequence is $T_s = 5\times10^{-5}$ seconds. The first four discrete prolate spheroidal sequences are generated and shown in Fig. 2. Their corresponding energy concentration is $\lambda_0 = 0.999\ 995$, $\lambda_1 = 0.999\ 730$, $\lambda_2 = 0.993\ 707$, and $\lambda_3 = 0.926\ 472$. So the first discrete prolate spheroidal sequence $v_0[k]$ achieves the optimal energy concentration in the frequency band $[-\Omega_0,\Omega_0]$.

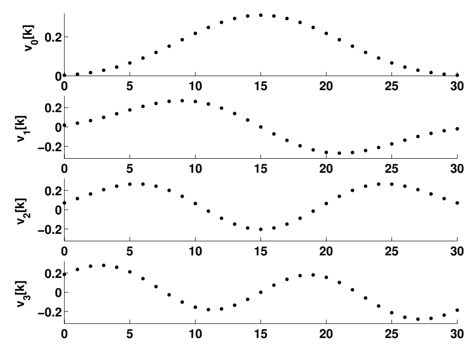

Fig. 2. Discrete prolate spheroidal sequences for the time duration 1.5×10^{-3} sec.

Since the initial and final values of the sequence $v_0[k]$ are not zero, the sequence $v_0[k]$ cannot be directly used as a robust vibration velocity profile. From the waveform of $v_0[k]$, it is clear that the $v_0[k]$ behaves like Gaussian functions such that the values decay sharply at the start and end points. So the sequence $v_0[k]$ can be vertically shifted down to make the start and end values to be zero,

$$vel[k] = v_0[k] - v_0[0], \quad k = 0,1,\cdots,N-1, \quad (12)$$

where N is the total data number of the sequence $v_0[k]$. Notice that $v_0[0] = v_0[N-1]$ because the sequence is a symmetric function. The sequence $vel[k]$, $k = 0, 1, \ldots, N-1$, can be used as a velocity profile. The resultant robust vibration suppression velocity profile is shown in Fig. 3. Depending on the rigid body position movement, the velocity profile must be multiplied with a constant. The discrete-time sequence of the acceleration profile $acc[k]$ can be generated from the discrete-time sequence of the velocity profile $vel[k]$ by

$$acc[k] = \frac{vel[k+1] - vel[k]}{T_s}, \tag{13}$$

where T_s is the sampling period.

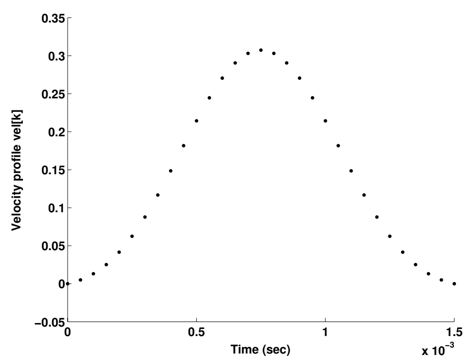

Fig. 3. A robust vibration suppression velocity profile from discrete prolate spheroidal sequence $v_0[k]$ with the move time 1.5×10^{-3} sec.

The vertically shifted discrete prolate spheroidal sequence $vel[k]$ slightly impairs its energy concentration. For the above example, the energy concentration measure $\beta^2(W)$ of $vel[k]$ is approximately 0.999 979. Compared with the optimal energy concentration value $\lambda_0 = 0.999\ 995$, the vertically shifted version of $v_0[k]$, i.e. $vel[k]$ only loses a slight amount of energy concentration. With the decrease of the move time, the difference of the energy concentration measure between $v_0[k]$ and $vel[k] = v_0[k] - v_0[0]$ will increase. Fig. 4 shows the difference of the energy concentration measure $\beta^2(W)$ between $v_0[k]$ and $vel[k] = v_0[k] - v_0[0]$ from the move time 0.5×10^{-3} seconds to move time 1.5×10^{-3} seconds. It shows that at the time duration of 0.5×10^{-3} sec, the difference of the energy concentration measure between $v_0[k]$ and $vel[k] = v_0[k] - v_0[0]$ is about $0.958 - 0.888 = 0.070$. The significant difference is caused because the initial and final values of the optimal energy concentrated DPSS $v_0[k]$ are very large. For the time duration of 0.5×10^{-3} sec, the resultant $v_0[k]$ with the same frequency band Ω_0 is shown in Fig. 5. It clearly shows that the initial and final values of the discrete sequence $v_0[k]$ decay slowly, so the choose of time duration of the discrete sequence as 0.5×10^{-3} seconds is not suitable to suppress all the resonance frequency ($\geq \Omega_0 = 9.68 \times 10^3$ rad/sec) modes in a flexible system. The plot of energy concentration measure with respect to the time duration gives a tradeoff between energy concentration measure and time duration when the first resonance frequency Ω_0 and the sampling period T_s are determined.

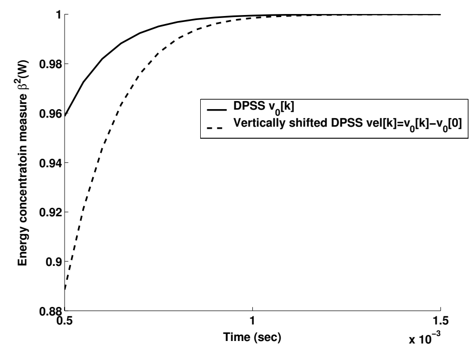

Fig. 4. The difference of the energy concentration measure $\beta^2(W)$ between $v_0[k]$ and $vel[k] = v_0[k] - v_0[0]$.

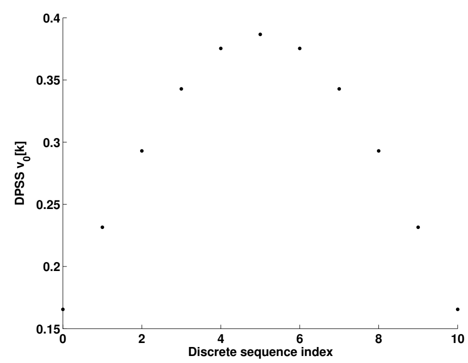

Fig. 5. DPSS $v_0[k]$ with the time duration 0.5×10^{-3} sec.

Notice the second optimal energy concentrated discrete prolate spheroidal sequence $v_1[k]$ in Fig. 2 can be directly used as an acceleration profile. From computation, the resultant velocity profile is approximately the same as $vel[k]$ in the sense of energy concentration in the frequency band $\omega \leq |\Omega_0|$.

IV. Simulation Results of Hard Disk Drive Short Seek Control

Consider the flexible system which is embedded in a hard disk assembly, $H(s) = K_c \cdot K_v \cdot K_p \cdot R(s) \frac{1}{s^2}$, where the input is the current signal in amps and the output is the position signal in tracks. The variable $K_c = 8.125$ $\frac{\text{tracks/sample}^2}{\text{amp}}$ is a constant gain from current to acceleration, $K_v = 2 \times 10^4$ $\frac{\text{samples}}{\text{sec}}$ is the velocity gain, $K_p = 2 \times 10^4$ $\frac{\text{samples}}{\text{sec}}$ is the position gain, and $R(s)$ is a 28^{th} order resonance structure. The Bode magnitude plot of $R(s)$ is shown in Fig. 6. This transfer function was derived from the flexible arm of an open disk drive at the Oklahoma State University Advanced Controls Laboratory. The resonance modes change drastically due to variation of the mode parameters. On the Bode plot, the peaks of the frequency response may shift both in frequency and in amplitude.

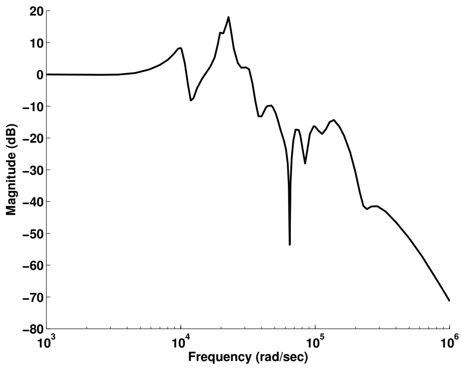

Fig. 6. Bode magnitude of the resonance structure.

With parameters settings $\Omega_0 = 9.68 \times 10^3$ rad/sec, the move time of 2.5×10^{-3} sec, and the sampling period of $T_s = 5 \times 10^{-5}$ sec, the zeroth order DPSS $v_0[k]$ is used to design the control input signal for a 100-track seek. Fig. 7 shows the current signal. Fig. 8 shows the position signal. Fig. 9 shows the position signal near the target track. It shows that the position signal settles within $\pm\frac{5}{100}$ track immediately after the move time of 2.5×10^{-3} sec. So the current signal suppresses the residual vibration induced by all the high frequency resonance modes. Now, the current signal is analyzed from the filter point of view. Fig. 10 shows the reference velocity signal. This signal is treated as the impulse response of a Finite Impulse Response (FIR) filter. The magnitude of the frequency response of this FIR filter is shown in Fig. 11. It is clear that this FIR filter has a superior cutoff of high frequency signals.

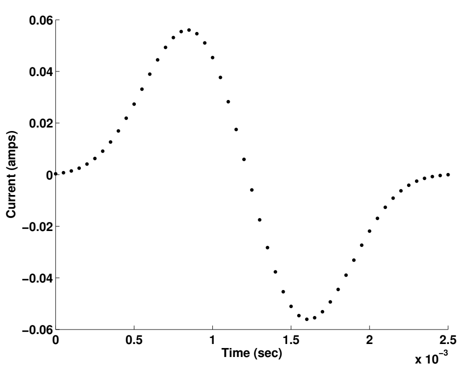

Fig. 7. Current control input signal.

It must be noted that the control input move time cannot be arbitrarily reduced if a certain seek time is required. It depends on the resonance characteristics. As shown in [1], a signal is not able to arbitrarily achieve both time and frequency localization. Reducing move time will result in a poor frequency concentration. Fig. 12 shows the concentration $1 - \beta^2(W)$ of the current control input with different move time for the same sampling period and first resonance frequency given before. From Fig. 12, if the move time of the control input is chosen to be 0.5 msec, the minimal

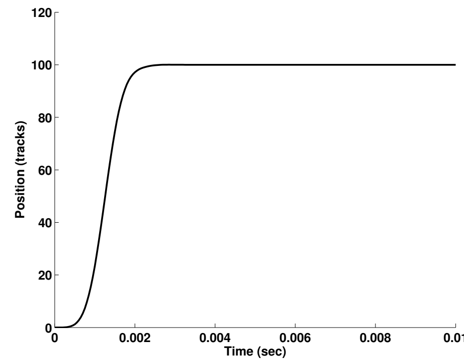

Fig. 8. Position signal.

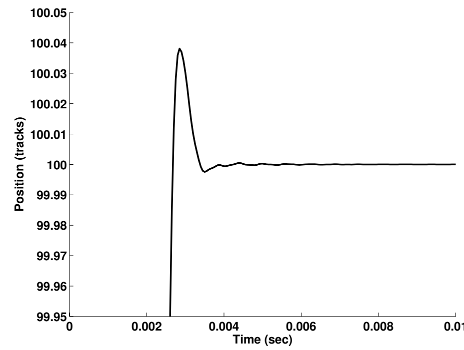

Fig. 9. Position signal near the target track.

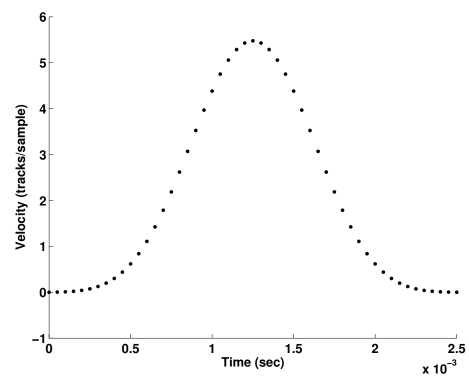

Fig. 10. Reference velocity signal.

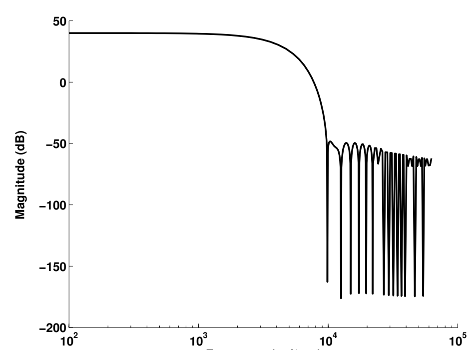

Fig. 11. Frequency response of the FIR filter whose impulse response is the reference velocity signal.

proportion of its energy after the first resonance is about 0.4 which is very poor. There is a tradeoff between the move time of a control input and its concentration in the frequency domain as shown in Fig. 12.

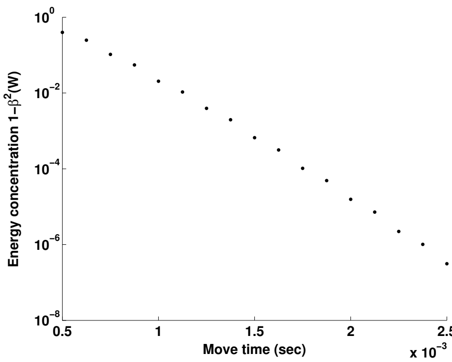

Fig. 12. Concentration $1-\beta^2(W)$ of current control input with different move time.

V. Conclusions

In this examination, a control profile is generated which suppresses all the high frequency resonant dynamics in a flexible dynamic system. This control profile is based on the shifted prolate spheroidal wave function that optimally achieves the energy concentration property. In a practical system, a lower resonance frequency mode may exist which is located far from the high frequency resonance modes as shown in Fig. 13. If the low frequency Ω_1 in Fig. 13 is chosen to be a bandwidth for the vibration suppression control profile generation, the time duration of the control profile is inefficiently increased. To suppress a specific low frequency resonance mode, the technique of low frequency vibration suppression shape filter is proposed in [11]. In [11], it shows that both the Input Shaping®[1] [12] and OATF [13] are special cases of a non-continuous function based vibration suppression shape filter. Different from the Input Shaping® and OATF, the vibration suppression shape filter in [11] is generated from a continuous function, so it is able to suppress the high frequency resonance modes besides canceling the low frequence resonance modes if the shape filter is designed based on a low frequency resonance mode. However, the Input Shaping® and OATF are not able to suppress the unmodeled high frequency vibrations if they are designed based on a low frequency resonance mode [11]. Combination of the methods in [11] and the methods in this paper generates a vibration suppression control profile that is able to suppress all the resonant dynamics in a flexible system [14]. Experimental results of hard disk drive actuator short seek control with both the methods in this paper and Input Shaping® are reported in [14]. For hard disk drive long seek control, both acceleration (or drive current) and velocity constraints should be considered. The vibration suppression control profile generation with both acceleration and velocity constraints is studied in [15].

[1]Input Shaping® is a registered trademark of Convolve, Inc. in the United States.

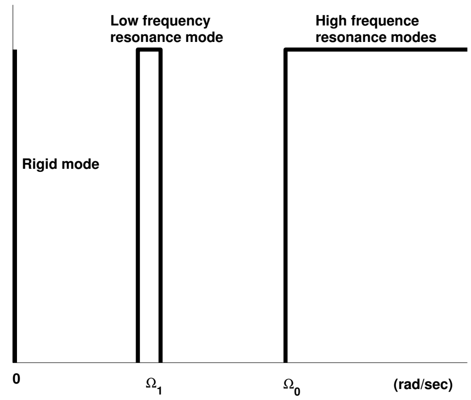

Fig. 13. Illustration of existence of a low resonance frequency mode located far from the high frequency modes in a flexible system.

The methods in this paper are patented (pending). Commercial use of these methods requires written permission from the Oklahoma State University.

References

[1] L. Zhou and E. A. Misawa, "Robust vibration suppression control profile generation based on time-frequency uncertainty," in *Proceedings of the American Control Conference*, Boston, MA, 2004.

[2] D. Slepian and H. O. Pollak, "Prolate spheroidal wave functions, Fourier analysis and uncertainty, I," *The Bell System Technical Journal*, vol. 40, no. 1, pp. 43–64, 1961.

[3] H. J. Landau and H. O. Pollak, "Prolate spheroidal wave functions, Fourier analysis and uncertainty, II," *The Bell System Technical Journal*, vol. 40, no. 1, pp. 65–84, 1961.

[4] ——, "Prolate spheroidal wave functions, Fourier analysis and uncertainty, III," *The Bell System Technical Journal*, vol. 41, no. 4, pp. 1295–1336, 1962.

[5] D. Slepian, "Prolate spheroidal wave functions, Fourier analysis and uncertainty, IV," *The Bell System Technical Journal*, vol. 43, no. 6, pp. 3009–3058, 1964.

[6] ——, "Prolate spheroidal wave functions, Fourier analysis and uncertainty, V: The discrete case," *The Bell System Technical Journal*, vol. 57, no. 5, pp. 1371–1430, 1978.

[7] R. Courant and D. Hilbert, *Methods of Mathematical Physics, Vol. 1*. Interscience Publishers, New York, 1955.

[8] D. B. Percival and A. T. Walden, *Spectral Analysis for Physical Applications - Multitaper and Conventional Univariate Techniques*. Cambridge University Press, 1993.

[9] L. Zhou, "Robust vibration suppression control profile generation," Ph.D. dissertation, Oklahoma State University, 2005.

[10] Mathworks, *Signal Processing Toolbox for Use with MATLAB*, 2002.

[11] L. Zhou and E. A. Misawa, "From Input Shaping® and OATF to vibration suppression shape filter," accepted to the 2005 American Control Conference, Portland, OR.

[12] N. C. Singer, W. P. Seering, and K. A. Pasch, "Shaping command inputs to minimize unwanted dynamics," United States Patent, 4,916,635, April 1990.

[13] D. P. Magee and W. J. Book, "Optimal filtering to minimize the elastic behavior in serial link manipulators," in *Proceedings of the American Control Conference*, vol. 1, 1998, pp. 2637–2641.

[14] L. Zhou and E. A. Misawa, "Low frequency vibration suppression shape filter and high frequency vibration suppression shape filter," accepted to the 2005 American Control Conference, Portland, OR.

[15] ——, "Robust vibration suppression control profile generation with both acceleration and velocity constraints," accepted to the 2005 American Control Conference, Portland, OR.